Per. Mineral. (2004), *73*, 29-52 http://go.to/permin
SPECIAL ISSUE 1 : A showcase of the Italian research in petrology: magmatism in Italy

PERIODICO di MINERALOGIA
established in 1930

An International Journal of
MINERALOGY, CRYSTALLOGRAPHY, GEOCHEMISTRY, ORE DEPOSITS, PETROLOGY, VOLCANOLOGY
and applied topics on *Environment, Archaeometry* and *Cultural Heritage*

Genesis and evolution of Mt. Etna alkaline lavas: petrological and Sr-Nd-B isotope constraints

PIETRO ARMIENTI[1,2]*, SONIA TONARINI[2], MASSIMO D'ORAZIO[1,2] and FABRIZIO INNOCENTI[1,2]

[1] Dipartimento di Scienze della Terra, Università di Pisa, Via S. Maria 53, 56126 Pisa, Italy
[2] Istituto di Geoscienze e Georisorse, C.N.R., Via Moruzzi 1, 56124 Pisa, Italy

ABSTRACT. — Mt. Etna lies at the northern margin of the African plate, on the accretionary prism of the Africa-Europe subduction system. Differential roll-back of the Ionian oceanic lithosphere has created a vertical slab window through which the passive rise of asthenosphere causes partial melting and magma genesis. In this rapidly evolving geodynamic context, the increase of alkalinity in time, accompanied by variations of Sr and Nd isotopes, is a first order feature. Fluid mobile elements and B systematics reveal the fundamental role played by fluids released by the dehydrating oceanic lithosphere, even if they are added to the mantle source in amounts no larger than 1 wt.%. This induces relatively high H_2O contents in Etna magmas that exert a strong control on phase relationships. Compositions of alkaline primary melts have been reconstructed and used to constrain the depth of origin and fractionation sequences at various pressures. It was found that phase relations at the crust-mantle boundary can only produce basaltic compositions akin to the less evolved sub-aphyric lavas, whereas trachybasaltic compositions are generated in the depth range 12-3 km together with cumulate bodies detected through geophysical investigations and here related to massive pyroxene and plagioclase fractionation. Detailed monitoring of Sr-isotope equilibrium between pyroxene and host rock revealed both the increase of $^{87}Sr/^{86}Sr$ over time and the occurrence of mixing processes between distinct batches of magma in the plumbing system. Sr, Nd and B systematics also reveal contamination effects due to interactions with lower crust and sporadic interaction with the sedimentary basement.

RIASSUNTO. — Il Monte Etna sorge sul margine settentrionale della Placca Africana, sul prisma di accrezione del sistema di subduzione tra Africa ed Europa. Il roll-back differenziale della litosfera oceanica Ionica induce la comparsa nella regione Etnea di una finestra astenosferica a sviluppo verticale, attraverso la quale è possibile la risalita passiva dell'astenosfera e la sua conseguente fusione parziale. In questo contesto geodinamico in rapida evoluzione, l'alcalinità dei magmi eruttati subisce un marcato incremento nel tempo, accompagnato da variazioni regolari della composizione isotopica di Sr e Nd. La composizione isotopica del boro, la sua abbondanza e quella degli altri elementi mobili nella fase fluida, rivelano il ruolo fondamentale giocato dai fluidi rilasciati dalla litosfera Ionica in via di deidratazione. Anche se questi vengono aggiunti alla sorgente mantellica in ragione di non più dell'1% in peso, ciò induce più basse temperature di solidus nel mantello ed elevati contenuti di acqua nei prodotti della sua fusione parziale. Gli elevati tenori di H_2O esercitano un forte controllo sulle relazioni di fase durante la successiva risalita dei magmi Etnei. Le

* Corresponding author, E-mail: armienti@dst.unipi.it

composizioni dei fusi primari sono state ricostruite ed usate per definirne le profondità di origine e le sequenze di frazionamento a varie pressioni. Le relazioni di fase alla profondità della transizione crosta-mantello sono tali da produrre liquidi di composizione basaltica, simili alle lave primitive sub-afiriche; al contrario le composizioni dei liquidi trachibasaltici, che di norma alimentano l'attività effusiva ed esplosiva del vulcano, sono raggiunte dai magmi in risalita in un intervallo di profondità compreso tra 12 e 3 km. La loro genesi è correlata ad un cospicuo frazionamento di pirosseno e plagioclasio, responsabile anche della formazione degli estesi corpi cumulitici rilevati dall'indagine geofisica. Il monitoraggio dell'equilibrio isotopico dello Sr tra clinopirosseni e roccia totale, ha rivelato sia l'incremento nel tempo del rapporto $^{87}Sr/^{86}Sr$, sia la presenza di processi di mixing tra distinte masse di magma nel sistema di alimentazione del vulcano. Gli isotopi di Sr, Nd e B mostrano altresì il ricorrere di episodi di contaminazione, per lo più causati da interazioni con la crosta inferiore o, sporadicamente, dovuti ad apporti del basamento sedimentario.

KEY WORDS: *Mt. Etna, alkaline lavas, Sr-Nd-B isotopes, petrology, geochemistry, geodynamics*

INTRODUCTION

Owing to its almost continuous and well-documented eruptive activity during the past two millennia, its easy access and repeated civil defense emergencies, Mt. Etna is a world-famous laboratory volcano for studying magma dynamics, eruptive mechanisms, differentiation processes and for testing theoretical models. The peculiar geodynamic context within which Mt. Etna occurs (Fig. 1), coupled with a continuous record of erupted products, has stimulated many geochemical and isotopic researches aimed at constraining the origin and the evolution of magmas. Over time scales varying from 10^5 to 10^1 years, Mt. Etna exhibits changes of chemical and petrographical features of erupted products that are linked to processes of deep and shallow origin. A dominant role is played by the depth of partial melting in the mantle source and by the effects of P-T-P_{H_2O} conditions on the relevant liquidus phase relations.

Most of the geochemical and geophysical studies carried out on Etnean magmatism focused on the recent and current eruptions with the following main goals:

a) To identify the nature and phase relations of the differentiation and/or assimilation processes that the magmas experienced;

b) To evaluate the location and size of the system in which differentiation occurs (magma chamber/s)

c) To evaluate the compositions of primary magmas and their conditions of formation with respect to geochemical features of the mantle source.

The magmatic evolution of the Mt. Etna volcanic system has been described by many authors (e.g.: Carter and Civetta, 1977; Tanguy, 1978; Joron and Treuil, 1984; Chester *et al.*, 1985; Condomines *et al.*, 1995; D'Orazio, 1993; Chester, 1993; Kamenetsky and Clocchiatti, 1996; Tanguy *et al.*, 1997). The influence of fluids in the genesis of recent Mt. Etna magmas has been also the subject of detailed investigations (e.g.: Métrich and Clocchiatti, 1989; Allard *et al.*, 1991; Métrich and Rutherford, 1998; Schiano *et al.*, 2001; Tonarini *et al.*, 2001). In the recent literature (Schiano *et al.*, 2001; Tonarini *et al.*, 2001), it has been suggested that asthenosphere upwelling initially caused melting in the mantle beneath Etna, while fluids released by the subducting Ionian slab have imprinted a progressive signature of enrichment in fluid mobile elements on the Etnean products. According to Gvirtzman and Nur (1999) and Doglioni *et al.* (2001), this context is created by a different rate of roll-back between the subducting Ionian (oceanic) lithosphere and the adjacent Sicilian (continental) crust, which induced asthenosphere diapirism through the resulting slab window (Fig. 1).

The aim of this work is to assess the relative role played by crustal level processes versus mantle source effects in the origin of the variability of Etnean magmas. This is obtained by recognizing a few fundamental processes whose recursive effects are able to explain the wide range of petrological and geochemical features.

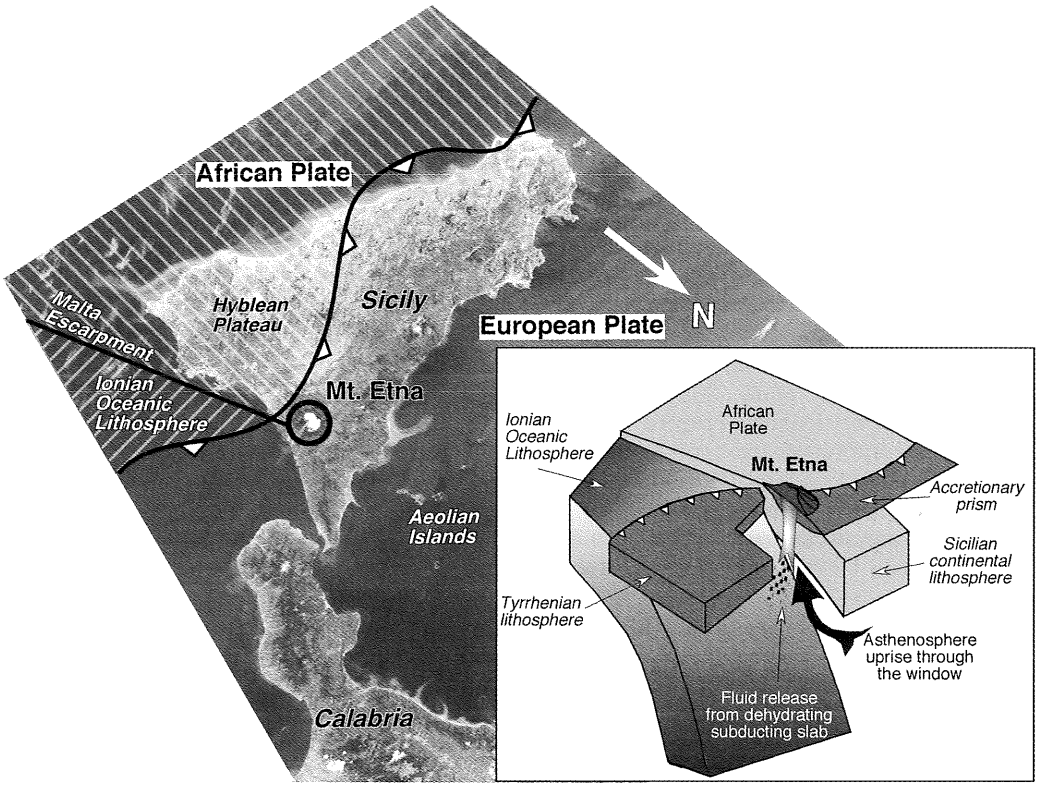

Fig. 1 – Geodynamic setting of the converging system between the African and European plates in the Sicily – Southern Tyrrhenian region. Inset: cartoon showing the Ionian-Sicilian subduction zones (modified after Gvirtzman and Nur, 1999 and Doglioni *et al.*, 2001). Roll-back of the subducting Ionian slab is responsible for passive asthenospheric rise through a vertical slab window below Mt. Etna.

GEODYNAMIC OUTLINES

The Mt. Etna volcanic complex is located on the east coast of Sicily (Fig. 1), where three different structural domains are in contact: i) the oceanic Ionian lithosphere to the east, considered as an old remnant of Mesozoic Tethys, ii) the relatively undeformed northern margin of the African Plate (Hyblean Plateau) to the south and iii) the corrugated collision zone between the European and African plates (Apennine-Maghrebian Chain) to the north. The geodynamic complexity of this area is further demonstrated by the occurrence, to the north and east of Mt. Etna, of lithospheric subduction related to the active Aeolian calc-alkaline volcanic arc and, to the south, by the occurrence of a widespread Cretaceous-Pleistocene basaltic magmatism outcropping on the Hyblean Plateau. Deep wells drilled on Hyblean Plateau indicate the presence of Na-alkaline basaltic magmatism, with typical intraplate signature, back to Middle Triassic time (Longaretti and Rocchi, 1992).

The volcanic history in the Etnean area probably began at about 500 ka (Condomines *et al.*, 1982; Gillot *et al.*, 1994) when both submarine and subaerial tholeiitic lavas were erupted in the so-called «Pre-etnean Gulf». Following this, a series of large central

volcanoes, of which Ellittico and Mongibello are the most recent, were built up during the northward migration of the eruptive axis. The erupted lavas gradually changed composition from subalkaline towards Na-alkaline (Fig. 2). The whole Etnean volcanic history was dominated by basaltic s.l. and slightly differentiated compositions (mainly alkali basalts-hawaiites-mugearites), although from time to time, the structural setting of the volcano allowed magma ponding at shallow crustal levels and the production of differentiated magmas up to trachytes, (Chester *et al.*, 1985; D'Orazio *et al.*, 1997). Typically, over the last three decades, erupted products have been buffered to trachybasaltic compositions (Tanguy and Clocchiatti, 1984; Tonarini *et al.*, 1995; Armienti *et al.*, 1996).

The following discussion is based on a data set of more than 1100 samples collected by the authors, for which 758 XRF analyses of major and trace elements are available (Pisa University's Dipartimento di Scienze della Terra), 150 ICP-MS analyses of 34 trace elements (Pisa University's Dipartimento di Scienze della Terra), and more than 100 coupled determinations of Sr-Nd isotopic compositions (IGG - CNR, Pisa; Appendix 1 and 2). Analytical procedures are reported by D'Orazio (1995) and Tonarini *et al.* (2001).

OUTLINES OF PETROGRAPHIC AND GEOCHEMICAL FEATURES OF ETNEAN LAVAS

On the basis of geological, volcanological and petrological constraints five distinct associations can be recognized:

1) *Tholeiitic basalts.* These rocks outcrop at the base of the volcanic succession, as isolated subaerial and subaqueous lava flows; they have also been dredged offshore from the nearby Ionian sea floor (Coltelli *et al.*, 1997). The analyzed samples are ol-hy normative, with Mg# between 59 and 69 and MgO contenst between 6.9 and 10.3 wt.%. Cr and Ni abundances are in the range 236-492 and 100-209 ppm, respectively. The average of K_2O is

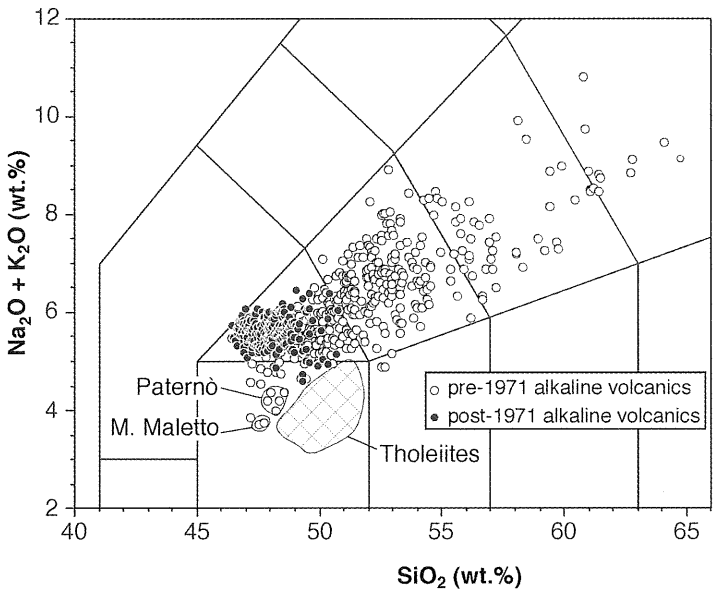

Fig. 2 – Total alkali vs. silica diagram for Mt. Etna volcanics. Since 1971 the compositions of erupted lavas are mainly confined within the trachybasalt field.

0.34% (0.18-0.66%) and K_2O/Na_2O ratio is 0.1 (0.05-0.2). They are characterized by a low porphyritic index with phenocrysts of olivine ± plagioclase ± clinopyroxene. Detailed descriptions of their mineralogy are reported by Tanguy (1978). Primitive mantle-normalized trace element patterns are characterized by enrichments in the most incompatible elements but Cs, Rb and K show a negative anomaly (Fig. 3a). Chondrite-normalized REE patterns show LREE enrichment (La_N = 61-97) and $[La/Lu]_N$ ratio 5.8-10.1.

2) *Ancient alkaline lavas.* This group comprises alkaline lavas often associated with the tholeiitic products and outcropping at the base of the main central volcanoes. Their chemical composition ranges from alkali basalts to mugearites. The association includes mainly porphyritic lavas of hawaiitic compositions with the mode dominated by plagioclase and pyroxene phenocrysts ± olivine ± Ti-magnetite. Some lavas with a low porphyritic index show a reversed Plg/Cpx modal ratio and a few of them carry ultramafic xenoliths. Among these the alkali basalts from the Paternò neck are the least evolved of our data set; their mantle-normalized trace element patterns show negative anomalies of Cs, K and Ti (Fig. 3b). The REE patterns are LREE-enriched (La_N = 103-152) with a $[La/Lu]_N$ ratio between 11 and 21.

3) *Valle del Bove volcanic succession.* This group includes a composite spectrum of Mt. Etna lithologic types: hawaiite, mugearite, benmoreite and trachyte lavas with both low (<5 vol.%) and high (>40 vol.%) phenocryst contents. Primitive volcanics are absent in this group whose chemical variability is mainly attributed to fractionation occurring at crustal level (D'Orazio *et al.*, 1997). Mantle-normalized incompatible element patterns share the general shape observed among the ancient alkaline lavas (Fig. 3b).

4) *Eccentric (parasitic) eruptions.* Rocks of this group are mainly alkali basalts and trachybasalts related to 338 monogenetic cinder cones of varying ages (Mazzarini and Armienti, 2001); most of them belong to historic eruptions. Parageneses are similar to the other alkaline

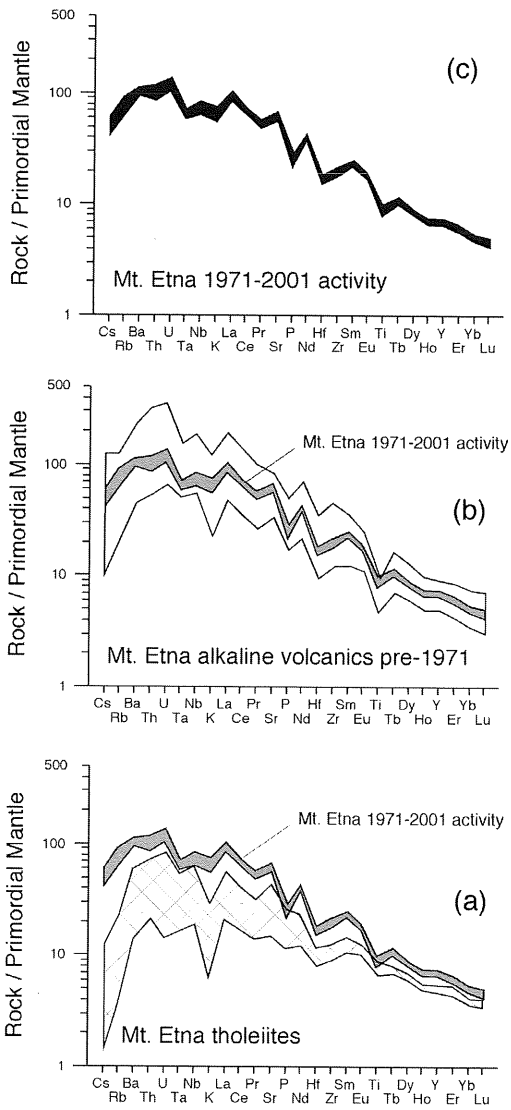

Fig. 3 – Primordial mantle – normalized incompatible element distributions for Mt. Etna tholeiites (a), pre-1971 (b) and post-1971 (c) alkaline lavas. Normalizing values after McDonough and Sun (1995).

important variations both within a single eruption and between different eruptions (Armienti *et al.*, 1984). Geochemical variations have been ascribed to major changes of the mantle source of the magmas, although a shallow level

lavas described above, (plg>cpx>ol ± sp), but this group also includes a number of sub-aphyric lavas that are among the least evolved of the volcano. The modes of the sub-aphyric basalts are often dominated by olivine and clinopyroxene whereas plagioclase is confined to the groundmass. Most of them were erupted after the formation of the Ellittico caldera, dated at about 15 ka (Gillot *et al.*, 1994). The high Mg# (56-63), low alkali content and trace element patterns testify to their relatively low degree evolution. Alkali basalt lavas from the base of Mt. Maletto parasitic cone are among the most primitive ever erupted during the alkaline cycle at Mt. Etna. Detailed petrographic and geochemical data on these rocks are reported by Armienti *et al.* (1988).

5) *Historic and current terminal and sub-terminal eruptive activity*. Since the Roman Age the volcanic activity underwent major changes in the composition and petrologic features. Though dominated by trachybasaltic compositions, lavas may show dramatic differences in modal compositions. Among the products erupted before the huge eruption of 1669, lavas dominated by plagioclase phenocrysts are frequent (*Cicirara* lavas, plg> 30 vol.%) (Armienti *et al.*, 1997). They have very little groundmass clinopyroxene and rare or absent olivine. The activity of the XVII century was characterized by the highest average output rate experienced by the volcano during its historic activity (1.19 m^3/sec; Hughes *et al.*, 1990). Since this period trachybasaltic lavas became dominant with a typical phenocryst paragenesis in which plg>cpx>olivine ± Ti-Mt. Since the XVII Century, K, Rb and Cs contents have started to rise. The increases are far more pronounced for activity after 1971 (hereafter considered as current activity) leading to a shift of K_2O/Na_2O ratio moving lava compositions into the field of potassic trachybasalts (Fig. 4) (Clocchiatti *et al.*, 1988; Armienti *et al.*, 1994).

The detailed time-controlled sampling available since 1983 has shown the occurrence of

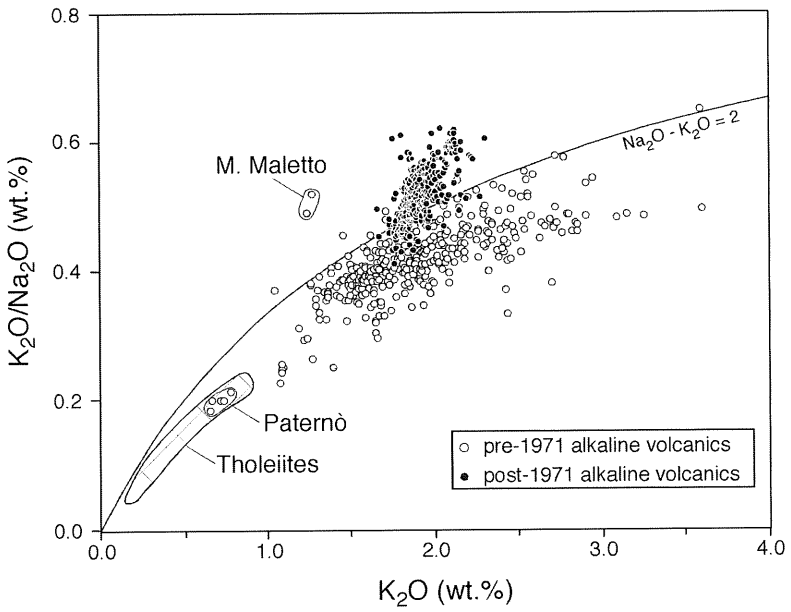

Fig. 4 – K_2O/Na_2O vs. K_2O diagram for Mt. Etna volcanics; the boundary line between sodic and potassic fields (Na_2O-K_2O = 2) is crossed by the post-1971 products.

selective contamination has been documented in some cases (Tonarini *et al.*, 2001).

PETROLOGICAL CONSTRAINTS

Primary melts

Trachybasalts are the prevalent volcanic products of Mt. Etna; their variability is related both to changes in the composition of primary melts and to P-T-PH_2O conditions during their evolution. Parasitic eruptions provide a conspicuous inventory of primitive products characterized by Mg-rich olivine as the first liquidus phase: systematic investigations of their glass inclusions indicate that the most Mg-rich olivines crystallized at temperatures around 1300°C and that the typical water content of trachybasaltic magma, before degassing, was around 2 wt.% (Métrich and Clocchiatti, 1989; Kamenetsky and Clocchiatti, 1996; Métrich and Rutherford, 1998). These data give the boundary conditions for assessing a range of possible primary compositions for Mt. Etna magmas. To achieve this goal, we selected the two least evolved, olivine-bearing sub-aphyric rocks: Paternò (an ancient alkaline lava) and Mt. Maletto (a pre-historic alkaline parasitic cone); in addition, we also selected a primitive basalt from the basal tholeiitic group (Biancavilla). These lavas have been checked for the stability of olivine as the first liquidus phase at different P (up to 1 GPa) and H_2O contents (0-2 wt.%) using the latest release of the pMelts code (Ghiorso *et al.*, 2002). Computations were performed at $\Delta QFM = +1$. Olivine was then added to re-equilibrate the magma with its mantle source (Fo_{90}) by using the olivine maximum fractionation equation (Pearce, 1978). Table 1 reports calculated primary melts that are high-Mg basalts close to picrites (Le Maitre, 2002). Their MgO content ranges from 11.3 to 13.2 wt.%, whereas their CaO/Al_2O_3 ratio varies between 0.51 and 0.64. The model compositions match those of glass inclusions with the highest MgO content and highest homogeneization temperature (T_{hom}) reported by Kamenetsky and Clocchiatti (1996). Compositional variability in natural and computed primary melts probably reflects a true variability within initial melts. This consideration is supported by the isotopic variation of erupted products (see below), by the compositional spectrum of erupted lavas and, last but not least, by the compositional variation of melt inclusions in Mg-rich olivines. Indeed, the occurrence of glass inclusions with different petrogenetic affinities (tholeiitic and alkali basaltic) in the olivine population of the same rock (Clocchiatti *et al.*, 1992) suggests that a magma batch can be produced by the aggregation of melts generated at different depths with different degrees of melting (aggregated melting).

Depth of the source region

Computed primary melts have been used to evaluate the depth of magma genesis by using a petrogenetic grid based on the reaction:

$$Mg_2SiO_4 + SiO_2 = 2\ MgSiO_3 \qquad (1)$$
$$\text{Ol} \quad \text{melt} \quad \text{Opx}$$

that controls the P-T dependence of silica activity in mantle melts (Ghiorso and Carmichael, 1987). Silica activity can be independently computed for primary melts by the regular solution model proposed by Ghiorso *et al.* (1983) in which a_{SiO2} is a function of composition and temperature (Fig. 5). The H_2O content was set to 1 wt.% on the basis of the estimation of water abundance in trachybasalts (about 2 wt.%; Métrich and Rutherford, 1998) and considering that about 50% by weight of gabbroic fractionation is needed to achieve trachybasaltic composition. Assuming that the primary melts have the same potential temperature as their mantle source, the T interval was constrained by T_{hom} of glass inclusions and ranges from 1250 to 1350°C (Clocchiatti *et al.*, 1992; Kamenetsky and Clocchiatti, 1996). With these boundary conditions, the petrogenetic grid suggests a depth of origin of 1.8-1.5 GPa (Fig. 5). These depths have to be considered as minimum depths of re-equilibration since the liquids

TABLE 1

Calculated primary melts of Mt. Etna and primitive glass inclusions in olivine phenocrysts

	A Biancavilla	B Mt. Maletto	C Paternò	D PMI-Mal12	E PMI-Pat
SiO_2 (wt.%)	48.51	46.65	48.23	44.95	48.64
TiO_2	1.33	1.28	1.43	1.53	1.40
Al_2O_3	15.63	14.80	16.55	14.41	14.92
Fe_2O_3	1.90	1.91	1.95		
FeO	8.05	8.55	7.31	11.21	6.86
MnO	0.14	0.16	0.15	0.24	0.04
MgO	12.45	13.23	11.32	10.06	12.26
CaO	8.43	9.84	8.51	12.21	11.53
Na_2O	2.91	2.13	3.49	2.51	3.20
K_2O	0.32	1.10	0.64	1.23	0.50
P_2O_5	0.34	0.35	0.41	0.45	0.33
Ni (ppm)	300	130	277		
Ol added (wt. %)	10	15	1.6		
T_{lq} or T_{hom} (°C)	1222	1221	1260	1320	1335
P (Gpa)	0.8	0.8	0.8		

Columns A, B, C, are the compositions calculated by adding back in equilibrium olivine to the Biancavilla tholeiite basalt, Mt. Maletto and Paternò alkali basalts, respectively, until these magmas are in equilibrium with mantle olivine Fo90. Columns D, E are the compositions of primitive glass inclusions in Mt. Maletto and Paternò olivine phenocrysts (Kamenetsky and Clocchiatti, 1996). Ni content calculated on the base of variable partition coefficient D_{Ni}, according to Beattie et al. (1991). T_{lq} is the liquidus temperature computed at 0.8 GPa with 1 wt.% H2O. T_{hom} = homogenisation temperature (Kamenetsky and Clocchiatti, 1996).

collecting to form the magma batch keep the imprint of the last event of re-equilibration within the mantle matrix.

From primary melts to hawaiites

The transition from primary melts to trachybasalts has been explored using the pMelts code (Ghiorso *et al.*, 2002) at different P conditions, starting from the computed primary melts of Mt. Maletto and Paternò. These rocks encompass the whole chemical range of the most primitive lavas; the initial water content and fO_2 were assumed to be 1 wt.%, and ΔQFM+1, respectively. Since Mt. Etna lavas exhibit parageneses dominated by phenocrysts of plagioclase, clinopyroxene, olivine, ± spinel, the comparison between natural and calculated fractionation paths can be displayed on the CaO/Al_2O_3 vs. MgO diagram (Fig. 6) that tracks the changes in the fractionating assemblage. In fact, olivine fractination induces a large variation of MgO contents without affecting the CaO/Al_2O_3 ratio, whereas augite and plagioclase fractionation strongly influence the CaO and Al_2O_3 contents. In Fig. 6 sub-aphyric lavas with MgO > 6% fall on an almost horizontal trend, whereas more evolved rocks show a positive slope. Figure 6 also shows that pre-1971 lavas attain a degree of evolution that is reached by post-1971 products, which, in turn, display

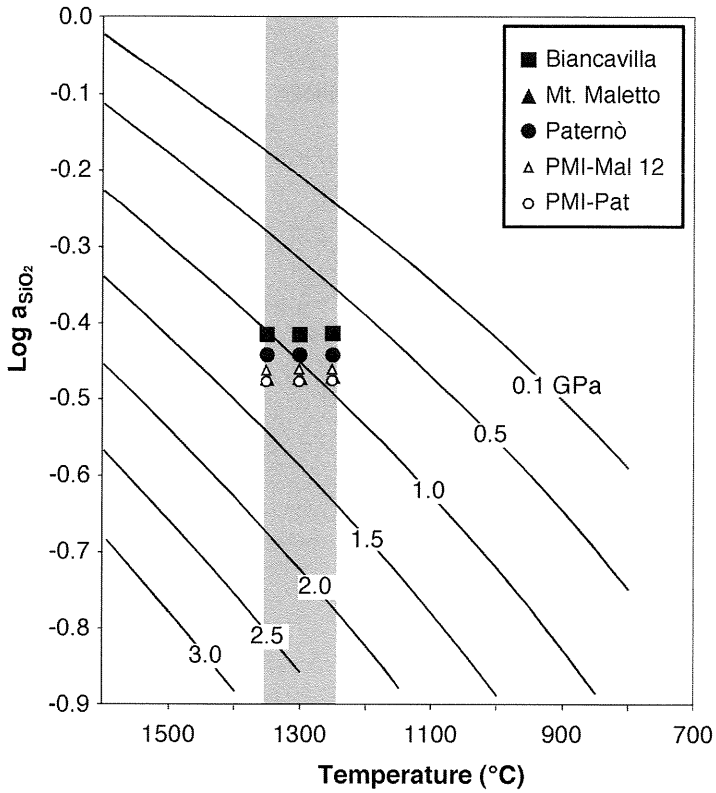

Fig. 5 – Silica activity vs. temperature (°C) at different total pressures (GPa) for the Mt. Etna primary melts reported in Table 1. Silica activity is computed at T = 1350, 1300 and 1250 °C with the regular solution model of Ghiorso *et al.*, (1995). The gray strip encompasses the maximum temperatures of equilibration measured in melt inclusion hosted in forsterite-rich olivines (Kamenetsky and Clocchiatti, 1996).

higher CaO/Al_2O_3 ratios at similar MgO contents.

On the basis of seismological evidence several authors have identified a high-velocity body below Mt. Etna between 12 and 3-5 km, and suggested also that its upper and lower boundaries represent levels of preferential magma ponding and differentiation (Laigle and Hirn, 1999; Murru *et al.*, 1999; Chiarabba *et al.*, 2000; Patanè *et al.*, 2003). Another major level of possible magma ponding is the mantle-crust boundary. Therefore fractionation paths have been modeled at different P values (0.8, 0.5 and 0.3 GPa) corresponding to the key depths of the Moho (20-25 km, Hirn *et al.*, 1997), the deepest portion of the high-velocity body (below 12 km) and its top (3-5 km).

The calculations use a temperature step of 5°C; the fractionation paths are reported in Fig. 6. They show, as a common feature, a first stage of olivine fractionation at constant CaO/Al_2O_3. At lower temperature, crystallization paths vary as a function of starting composition and pressure, but they always include a gabbroic fractionation interval (decreasing CaO/Al_2O_3 at decreasing MgO) that produces liquid lineages that mimic natural compositions.

The primary composition calculated for the Mt. Maletto magma is unable to yield liquids with the composition of Mt. Etna trachybasalts at

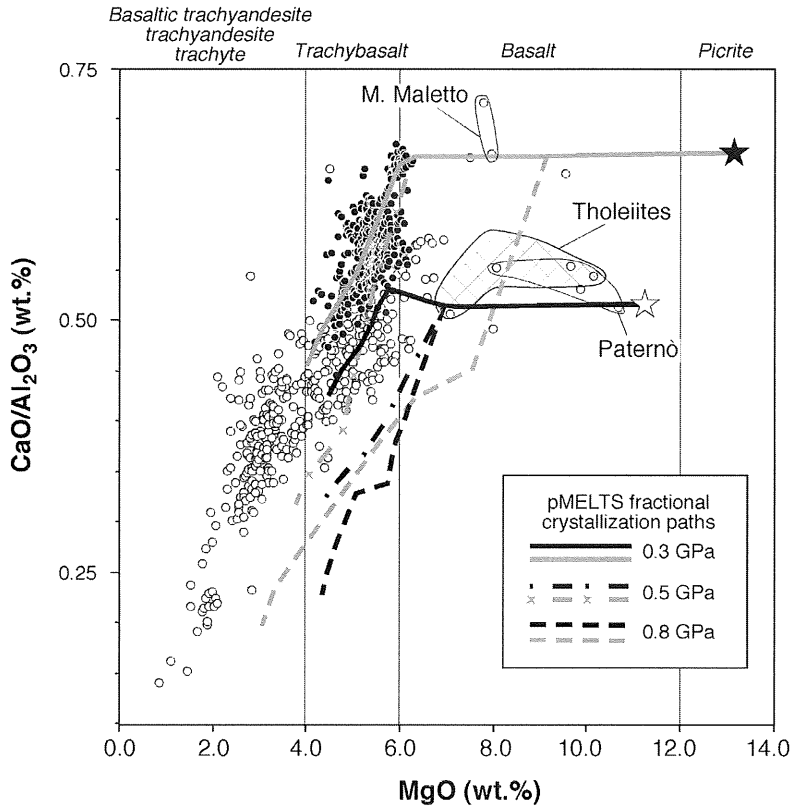

Fig. 6 – CaO/Al_2O_3 vs. MgO for Mt. Etna volcanics. Six fractional crystallization paths, simulated using the pMelts thermodynamic code (Ghiorso *et al.*, 2002), are also drawn in the diagram. Black and white stars are the calculated primary magmas of Mt. Maletto and Paternò, respectively. See text for further explanations.

P = 0.8 GPa. At this pressure, only basaltic compositions akin to some sub-aphyric lavas can be produced. This would imply a polybaric crystallization path to reach the fields of intermediate lava compositions. At lower pressures gabbroic fractionation starts at an MgO content typical of the less evolved trachybasalts and the computed trends in the interval 1150-1080°C overlap the array of natural compositions, both at 0.3 and 0.5 GPa. A relevant effect observed at 0.5 GPa is the massive crystallization of clinopyroxene (13 wt.%) and plagioclase (3 wt.%) in a small temperature interval (1150-1140°C). This is illustrated in Fig. 7a, b, where the cumulative amounts of fractionated solids are plotted against temperature. In the first stage of the evolutionary trend, olivine crystallizes at a rate of about 1 wt.% per 10°C, whereas when clinopyroxene and plagioclase appear after olivine, the mass crystallization rate increases by 15 times. This very high crystallization rate could be responsible for the formation of significant amounts of cumulus material in the plumbing system. Therefore the high-velocity, high-density body revealed by seismological investigations may be related to an attribute of the Mt. Etna magma phase diagram. The minor final kinks of the fractionation trends (Fig. 6) are related to the late occurrence of spinel on the liquidus.

In the fractionation paths of the Paternò primary melt, olivine is always a liquidus

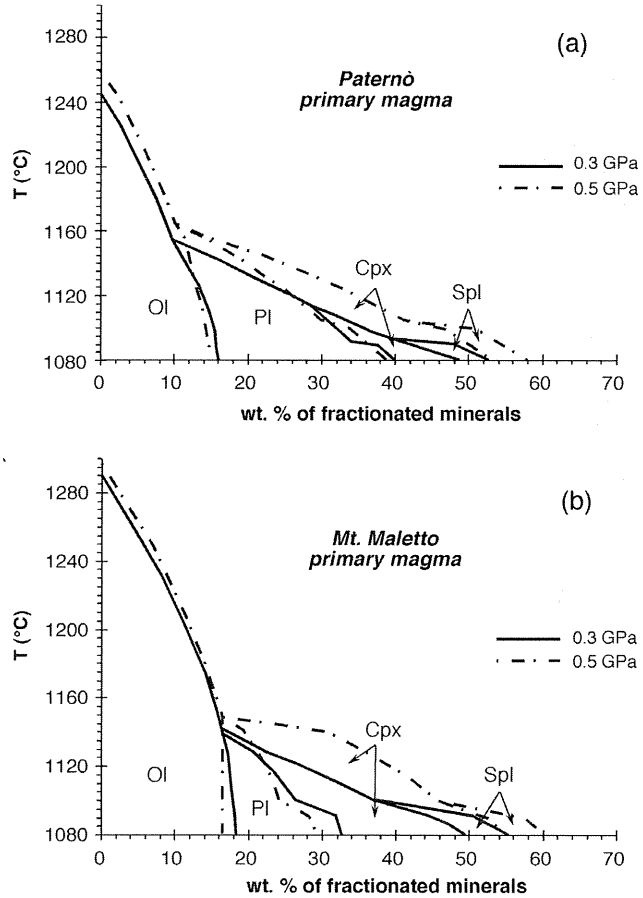

Fig. 7 – Temperature (°C) vs. cumulative amount of fractionated solids (wt.%) calculated with the pMELTS thermodynamic code for the crystal fractionation, at P = 0.3 and 0.5 GPa, of Paternò (a) and Mt. Maletto (b) estimated primary magmas. Phase abbreviations are Ol (olivine), Pl (plagioclase), Cpx (high-Ca clinopyroxene), Spl (spinel). Particular combinations of initial compositions and depth of ponding may yield plagioclase-dominated (a) or pyroxene-dominated (b) fractionated assemblages.

phase; furthermore, there is a gap between the liquidus temperatures of plagioclase and clinopyroxene (Fig. 7b). This melt, at 0.8 GPa, is unable to generate the observed trachybasaltic compositions. At 0.5 GPa the calculated path approximates the natural trend only for some MgO-rich trachybasalts; at this pressure, clinopyroxene appears at 1150°C, 10°C below plagioclase. At 0.3 GPa, there is a significant delay in the appearance of clinopyroxene on the liquidus. Thus, in the interval 1110°C < T < 1150°C only plagioclase joins olivine during fractionation, allowing Paternò-type initial melts to reach the compositional range of the dominant lavas of Mt. Etna (Fig. 7a). These particular combinations of magma composition and pressure of crystallization can explain the occurrence of «Cicirara» lavas, whose mode is dominated by plagioclase. These particular lavas were commonly erupted until the XVIII Century (Chester *et al.*, 1985; Armienti *et al.*,

1997) and are absent in XIX and XX centuries.

The described simulations are able to explain some conspicuous petrological features of magmatic evolution within the Etnean system. In particular, the occurrence of high mass crystallization rates between 0.3 and 0.5 GPa, in a temperature interval between 1150 and 1140°C, for suitable compositions of initial magmas (Mt. Maletto-like), is able to explain both the genesis of trachybasalts and the occurrence of high-density cumulates. Their density can be assessed on the basis of the cpx/plg ratio prevailing during the fractionation step that formed the dominant lavas of the volcano. Simulations yield a mass ratio of cpx/plg=11.5/2.5 corresponding to a cumulate density of 3.2 g/cm^3. Furthermore, taking into account the typical Vp ranges for clinopyroxene and plagioclase (7.7-7.4 and 6.7-6.4 km s^{-1}, respectively) and the correction due to P and T effects on Vp (dV/dP=1-1.5 km s^{-1} GPa^{-1}; -dV/dT= 2-4 10^{-4} km s^{-1} °C^{-1}; Farnetani *et al.*, 1996), it is possible to use the volume ratios of the cumulus phases to evaluate Vp in the high-density body. Assuming that at P = 0.5 GPa, T is 600 °C, the resulting Vp values are in the range 7.4-6.9 km s^{-1}, which can be compared with the value of 6.5 km s^{-1} reported by Chiarabba *et al.* (2000) in their seismological study of the plumbing system of Mt. Etna. The relatively high values found using our petrological modeling suggest that cumulate bodies probably do not form a continuous volume but are dispersed within lower density matrix (crystalline basement).

Particular compositions of initial melts (Paternò-like) associated with specific water contents can be characterized by a significant expansion of the plagioclase stability field. In terms of temperature, we could find a delay of about 50°C for appearance of clinopyroxene with respect to plagioclase. This last phase thus becomes the dominant phenocryst producing the mode of «Cicirara» lavas.

ISOTOPE CONSTRAINTS

Whole rock Sr, Nd and B isotope data

Sr and Nd isotope data for whole rocks are reported in Appendix 1 and Fig. 8. Some of the data have been already published by Tonarini *et al.* (1995), Armienti *et al.* (1996), D'Orazio *et al.* (1997) and Tonarini *et al.* (2001a).

$^{87}Sr/^{86}Sr$ ratio varies from 0.70304 to 0.70369 and $^{143}Nd/^{144}Nd$ ranges between 0.51297 and 0.512852. The tholeiitic basalts are characterized by the lowest Sr isotopic compositions (0.70304-0.70324) and highest $^{143}Nd/^{144}Nd$ (0.51297-0.51292) whereas the ancient alkaline lavas are transitional between tholeiites and the Valle del Bove lavas ($^{87}Sr/^{86}Sr$ = 0.70317-0.70343 and $^{143}Nd/^{144}Nd$ = 0.512925-0.512854). The primitive lavas from parasitic cones show a wide range between 0.70330 and 0.70369, and between 0.51290 and 0.51288 in Sr and Nd isotopic compositions, respectively. The historic and current summit activity is characterized by $^{87}Sr/^{86}Sr$ from 0.70340 to 0.70361 and $^{143}Nd/^{144}Nd$ from 0.51290 to 0.512852, with the highest Sr and lowest Nd isotopic ratios measured on the current activity.

The two isotope ratios are negatively correlated defining a main trend running from a depleted end-member (tholeiites) to the enriched recent alkaline lavas. However, starting from the main trend, we observe three second-order trends in which the negative correlation between $^{143}Nd/^{144}Nd$ and $^{87}Sr/^{86}Sr$ has a steeper slope (Fig. 8). The two limiting compositions adopted for petrological modeling of primary melts fall on the main trend, at opposite ends of the array described by the alkaline lavas.

Boron isotopic composition shows modest but significant variations ($\delta^{11}B$ = -8‰ to -3‰) that are well correlated with enrichments in fluid-mobile elements (FME) over other incompatible elements. Correlations of $\delta^{11}B$ with Sr and Nd isotope ratios and their temporal variations also occur (Fig. 9). The observed correlations have been considered as evidence of addition of a fluid component to an asthenospheric mantle source. The fluid responsible for the progressive

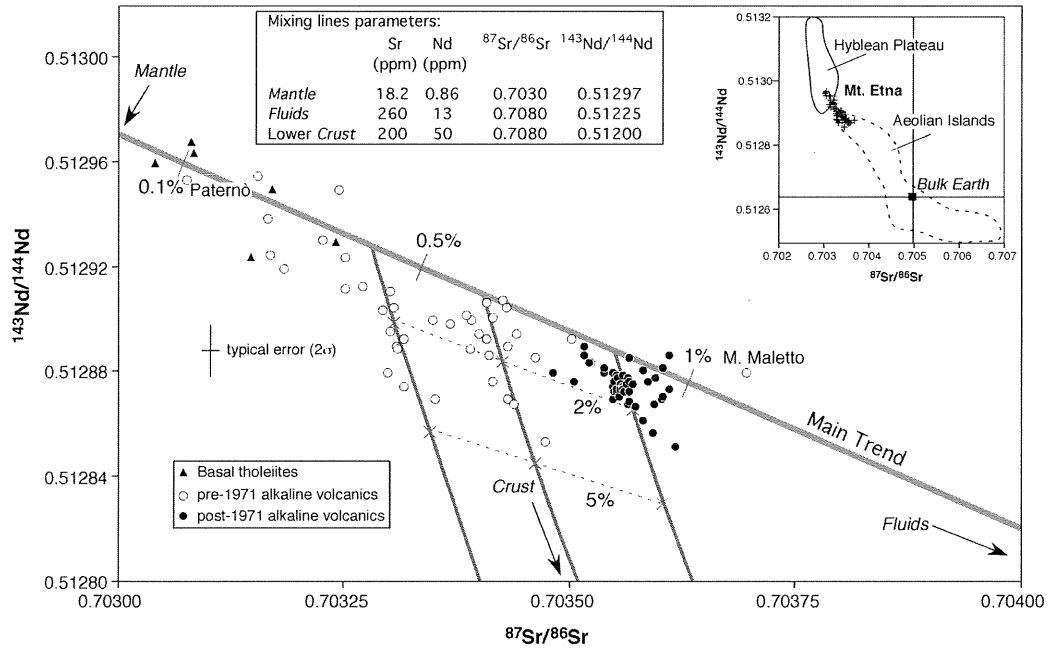

Fig. 8 – Sr and Nd isotope compositions of Mt. Etna volcanics. The Main Trend (thick gray line) is the mixing curve between a depleted mantle source and a slab-released fluid. Light gray lines are mixing curves between composition lying on the Main Trend and the lower continental crust. Dashed lines join points with the same amount of crustal contamination. Numbers on the mixing curves are the percent amount of enriched end-member (fluid or crust). In the inset are reported the data for Mt. Etna along with the fields of variation of the Hyblean Plateau and Aeolian Island (data from literature).

FME enrichment has been related to dehydration of the subducting Ionian oceanic slab (Tonarini *et al.*, 2001).

A simple binary mixing model between a slightly depleted mantle source and a subduction-related fluid phase fits the $\delta^{11}B$, $^{87}Sr/^{86}Sr$ and the FMEs enrichments very well and allows an estimate of the amount of subduction-related fluids involved in the genesis of Mt. Etna lavas of 0.1-1.0 wt.% (Tonarini *et al.*, 2001). The same model can explain the main trend observed in the Sr-Nd isotopic diagram. In fact, starting from the older alkaline lavas (Paternò), the main trend is matched by a binary mixing line between a pre-enrichment asthenospheric source with $^{87}Sr/^{86}Sr$ = 0.7030, Sr = 18.2 ppm (the same used for the boron model) and $^{143}Nd/^{144}Nd$ = 0.51297 and Nd = 0.86 ppm (Hofmann, 1988), and a fluid phase with Sr = 260 ppm, and Nd = 13 ppm (Sr/Nd = 20, as estimated by Tatsumi and Kogiso, 1997). The $^{87}Sr/^{86}Sr$ and $^{143}Nd/^{144}Nd$ ratios adopted for the fluid end-member are 0.7080 and 0.51225, respectively, within the range defined by typical values of an altered oceanic crust (Ishikawa and Tera, 1999) and those assumed for the sediments derived from the crust of the Calabrian arc (Caggianelli *et al.*, 1991).

B isotopes also indicate the occurrence of shallow level contamination effects that may decrease $\delta^{11}B$ on account of the interaction of Mt. Etna magma with the sedimentary basement. This process affects Mt. Maletto lavas that show a primitive composition coupled with $\delta^{11}B$, Sr isotopes and FMEs distribution modified by interactions with the sedimentary sequences beneath the volcano (Fig. 9; Tonarini *et al.*, 2001)

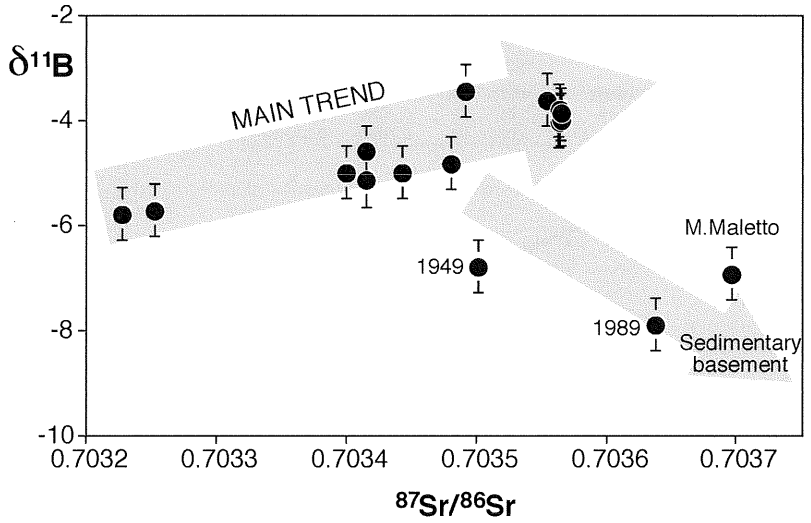

Fig. 9 – $\delta^{11}B$ vs. $^{87}Sr/^{86}Sr$ for Mt. Etna samples. Data on the large arrow, but M. Maletto, are from the Main Trend of Fig. 8. M. Maletto, 1949 and 1989 data are considered as the result of shallow selective contamination due to interaction with the sedimentary basement (detailed modeling in Tonarini *et al.*, 2001).

Clinopyroxene Sr isotopic data

The high water contents of Mt. Etna trachybasalts guarantee that clinopyroxene is an abundant early liquidus phase (Trigila *et al.*, 1990); this mineral can be easily separated to track shallow level processes possibly occurring after its crystallization. A check of Sr isotope equilibrium between whole rocks and separated clinopyroxene has been essentially focused on the current activity with some controls performed on key historic products. Fig. 10 reports Sr isotopic compositions of whole rocks (WR)-clinopyroxene pairs in temporal order for the current activity up to 2001. As a rule, clinopyoxenes, when found in disequilibrium, have a lower value of $^{87}Sr/^{86}Sr$ ratio with respect to their WR. The clinopyroxenes of lavas erupted before 1974 are equilibrated with their corresponding WR, with the exception of the 1910 and 1949 lavas. In these two samples the $^{87}Sr/^{86}Sr$ of the whole rock is higher than the other pre-1974 samples, while the cpx are close to the average values measured in whole rocks of the reference time span. Clinopyroxene phenocrysts of post-1974 products have more variable Sr isotopic compositions; those from 1974-1993 samples show a pronounced disequilibrium, whereas the following activity (1995-1999) shows uniform Sr isotopic ratios in WR and cpx, with a mean value of 0.70355. In particular, isotopic disequilibra found for Sr isotopes in 1991-1993 eruption have been explained as due to interaction between a prevailing magma and a residual mass with the isotopic signature of the previous activity (Tonarini *et al.* 1995, Armienti *et al.*, 1996); on the other hand, disequilibria in the lavas of the first two days of 1989 eruption are characterized by higher Sr isotope ratio of WR whereas Cpx overlaps with the average composition of the lavas erupted soon after (Fig. 10). Cpx-WR disequilibria in 1910, 1949 and 1989 have been interpreted as due to shallow level, pre-eruptive contamination processes (Tonarini *et al.*, 2001). After 1999 the Etnean system experienced a further increase of $^{87}Sr/^{86}Sr$ values of the summit activity products (WR data only) with a mean value of 0.70360.

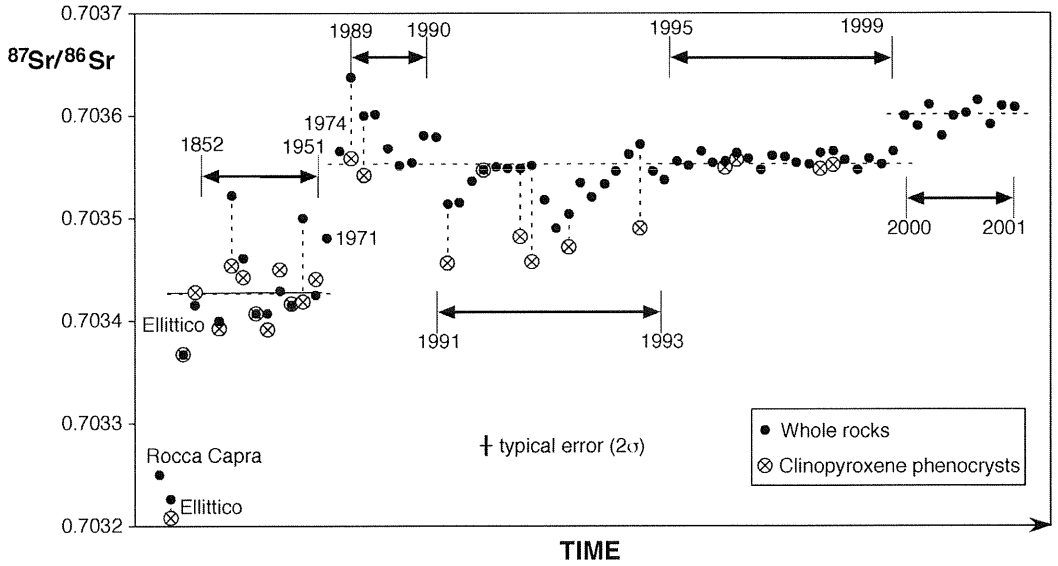

Fig. 10 – $^{87}Sr/^{86}Sr$ ratios of whole rocks and clinopyroxene phenocrysts of Mt. Etna volcanics arranged in temporal order (time scale not proportional). When cpx is in disequilibrium with the host rock, its Sr isotope composition is lower than total rock. The overall Sr isotope composition increases with time.

Summing up, data on WR and separated clinopyroxenes reveal how the increase of radiogenic Sr characterizing Mt. Etna during its whole history can be detected even on a scale of a few decades, so that the volcano is now fed by magma batches with distinct isotopic compositions compared to those supplied before 1974. In this general frame, shallow level processes such as crustal contamination and/or mixing between magma batches revealed by Cpx-WR disequilibria, contribute to a further variability of Sr isotopic composition of erupted lavas.

Summary and conclusions

Available data show a relatively wide petrological, geochemical and isotopic variability among Mt. Etna magmas. Several processes occurring between the source region and surface may act with different effects on the rising melts.

At the scale of the entire life span of the volcano, enrichment in alkalies with time is a first-order feature. This is accompanied by variation in Sr and Nd isotopic compositions that forms the main trend of Fig 8. The alkalinity enhancement over time essentially involves fluid mobile elements like Rb, Cs, B, K, implying an increase of the ratio between FMEs and incompatible immobile elements (e.g. Nb, Ta, Zr, Hf). Fig. 11 shows the positive correlation between $^{87}Sr/^{86}Sr$ and Rb/Nb ratio which documents the alkalinity evolution. This general scheme is confirmed by the progressive decrease of the $^{206}Pb/^{204}Pb$ ratio (Graham *et al.*, 1992). By contrast, other isotope compositons like those of He and O do not display a temporal shift (Marty *et al.*, 1994).

The enduring trend of increase in alkalinity, $^{87}Sr/^{86}Sr$ and $\delta^{11}B$ is linked to the evolving geodynamic context of Mt. Etna. The volcano is situated on the accretionary prism of the south Tyrrhenian subduction system and above a vertical slab window (Gvirtzman and

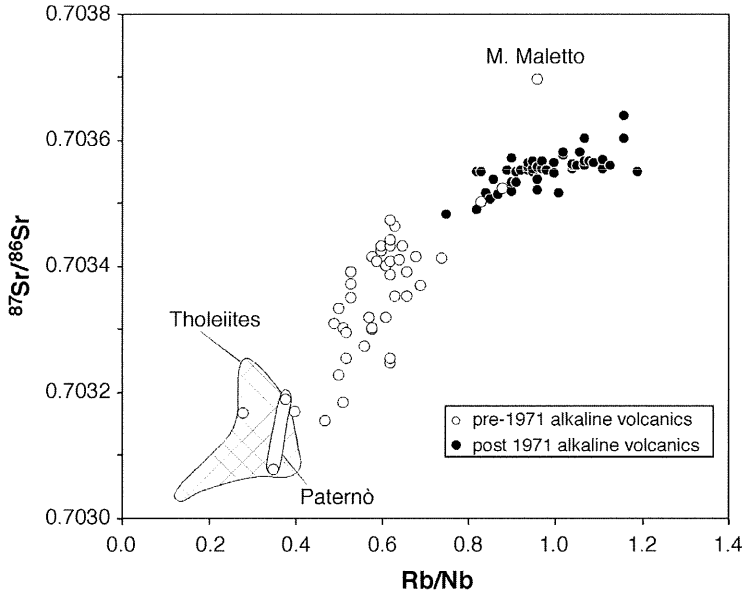

Fig. 11 – $^{87}Sr/^{86}Sr$ vs. Rb/Nb ratios for Mt. Etna samples. The positive correlation of the two ratios documents the temporal evolution of alkalinity.

Nur, 1999; Doglioni *et al.*, 2001). We interpret the peculiar geochemical and petrological evolution of Mt. Etna magmas as the effect of an increasing role of fluids released by the subducting Ionian oceanic crust enriching the mantle source. This latter is represented by asthenospheric mantle rising through the slab window and melting as a consequence of the combined action of pressure drop and fluid supply. Nearly pure asthenospheric melts are represented by the basal Etnean tholeiites which do not carry any imprint from the fluids derived from the subducting system. Indeed, their isotopic and geochemical signature is akin to that of Plio-Quaternary mafic magmas from the nearby Hyblean plateau (Trua *et al.*, 1998), erupted within the African foreland, well beyond any influence of the slab window.

Boron isotope data demonstrate that the fluid component is added in amount < 1 wt.% (Tonarini *et al.*, 2001). In this frame, the poorly variable O and He isotope compositions are due to the major element nature of oxygen and to the scarce variability of He isotopes in natural reservoirs (Anderson, 2001). A further evidence of the role of fluids in the genesis of Mt. Etna magmas is provided by the unusually high water content of the primary melts. Indeed, trachybasalts commonly feeding the volcano, exhibit pre-eruptive water contents around 2 wt.%, as documented by melt inclusion studies (Métrich and Clocchiatti, 1989). Although trachybasalts are the most common lavas, a small population of primitive basalts occurs in which olivine is the first liquidus phase, in a wide range of P, at high water content. This allowed determination of the composition of Mt. Etna primary melts which fall in the field of high-Mg basalts with MgO ranging between 11 and 13 wt.%. Mg#'s of calculated compositions are similar to the most primitive melt inclusions analyzed in Fo-rich olivine (Table 1). The minimum depth of re-equilibration of primitive melts with a lherzolitic mantle source (Ol=Fo90 and

Opx=En90) is around 1.5-1.8 GPa. This rather shallow depth of re-equilibration, when considered with the occurrence in the same olivine crystal of near-primary inclusions having different alkalinity, strongly suggests that aggregated melting may represent a key petrological process.

A further important process in the petrogenesis of Mt. Etna lavas is the dominant supply of trachybasaltic lavas to the eruptive activity. Starting from the defined set of alkaline primary melts, petrogenetic modeling indicates that a trachybasaltic composition can be obtained by fractionation of a gabbroic solid assemblage, in the pressure range of 0.3-0.5 GPa. Thermodynamic calculations show a massive crystallization of cpx when this phase joins or replaces olivine, which is the only liquidus phase in the early fractionation steps of primary melts (Fig. 6). The amount of cpx fractionated in a temperature interval of less than 10°C may be as large as 14 wt.% and contributes substantially to the growth of the high-density, high-Vp body imaged by seismologic investigations within the crust.

The trachybasalts may evolve during the rise to the surface due to further gabbroic fractionation and mixing. The gabbroic fractionation is suggested by modal variability of erupted products and is easily modeled by mass balance calculations (Armienti *et al.*, 1994); a major evidence for mixing is provided by the occurrence of cpx in isotopic disequilibrium with their host whole rocks.

As the processes of fractionation and mixing occur at crustal level, the interaction between magma batches and crustal materials may be envisaged as a further cause of variability. The effects of this kind of contamination are shown by the Sr-Nd isotope diagram, where steeper secondary trends depart from the main trend (Fig. 8). Second-order trends can be modeled as the interaction of melts from a time-evolving mantle source with crustal materials characterized by low Sr/Nd ratios (Sr/Nd = 4). The Hercynian intermediate-lower crust exposed in southern Calabria (Caggianelli *et al.*, 1991) fits this requirement with the only exclusion of metagabbroic rocks. Modeling suggests that the amount of crustal input is generally < 3%. The occurrence of distinct secondary trends suggests that, during its history, the volcano was not fed through an unique magma chamber in which refilling, assimilation and fractionation could develop, or, alternatively that the magma chamber was so small as to be rapidly influenced by new supply of magma.

Table 2 links the main features of Etnean lavas with specific physical processes. The relatively shallow genesis of primary melts is correlated to the occurrence of significant amounts of fluids derived from the subducting Ionian lithosphere; their interaction with mantle source is driven by the occurrence of a vertical slab window occurring in a unique geodynamic context. The subsequent evolution of magma develops in small-size systems that are able to record geochemical differences inherited by a source variably enriched in fluids + FME.

Two main steps characterize this evolution. The first, at the base of the crust, corresponds to the transition high-Mg basalt to alkali basalt due to olivine fractionation; the second develops at mid-crustal levels (9-15 km) and it is strictly controlled by the effects of water content on the phase relationships. In this step, intermediate lavas of trachybasaltic composition are generated as a result of massive gabbroic fractionation (cpx+pl±ol). Possible delay in the appearance of cpx on the liquidus can generate plagioclase-phyric intermediate lavas. The small size of shallow and deep reservoirs allows detection of geochemical and isotopic variations due to mixing and/or crustal contamination processes.

ACKNOWLEDGMENTS

Hilary Downes and Robert Clocchiatti are thanked for their critical reviews and Sandro Conticelli for the editorial assistance.

TABLE 2

Geochemical, petrographical and isotopic variations of Mt. Etna magmas and related processes

Observed features	Inferred process
Variable geochemical affinity of primary magmas (variation in H_2O content, alkalinity, Sr, Nd and B isotope ratios and arrangement of products along a main trend in the Sr-Nd isotope diagram)	Progressive involvement of a mantle source variably affected by fluid flux from the subducting Ionian slab
Last equilibration of primary melts with mantle at 1.5-1.8 GPa	Uprise of asthenosphere through a vertical slab window
Variable chemical affinity of melt inclusions in the same lava	Aggregate melting
Dominant supply of trachybasalts; occurrence of high Vp and high density body between 0.3-0.5 GPa	Massive crystallization of cpx between 0.3 and 0.5 GPa at high water content
Occurrence of plagioclase-phyric lavas (Cicirara)	Delay of cpx appearance on the liquidus as a consequence of the topology of phase diagram at given water content
Occurrence of secondary trends in the Sr-Nd isotope diagram	Crustal contamination at shallow level: crustal magma chambers do exist
Recurrent Sr isotope disequilibrium between cpx and whole rocks	i) Mixing among magmas with distinct source imprint: magma chambers must be small. ii) Occasional interaction with the sedimentary basement

APPENDIX 1

Sr-Nd isotope data for Mt. Etna volcanics

Sample	Material	$^{87}Sr/^{86}Sr$	± 2 σ_{mean}	$^{143}Nd/^{144}Nd$	± 2 σ_{mean}	Sample	Material	$^{87}Sr/^{86}Sr$	± 2 σ_{mean}	$^{143}Nd/^{144}Nd$	± 2 σ_{mean}
Basal tholeiitic lavas						*Current activity (post-1971)*					
Et-5	WR	0.70317	2	0.51295	3	e47 (1974)	WR	0.703564	13	0.512877	10
Et-7	WR	0.70324	6	0.51293	5	et.89.2 (1989)	WR	0.703637	13	0.512871	10
Et-104	WR	0.703080	11	0.512968	16	et89.5 (1989)	WR	0.703600	10	0.512871	10
Et-158	WR	0.70304	3	0.51296	2	SE-61 (1990)	WR	0.703580	16	0.512862	10
Et-167	WR	0.703147	10	0.512924	17	14.12.91 S (1991)	WR	0.703575	10		
Et-171	WR	0.703083	11	0.512964	19	14.12.91 L (1991)	WR	0.703579	10	0.512881	10
						15.12.91 (1991)	WR	0.703513	10		
Ancient alkaline lavas						18.12.91 A (1991)	WR	0.703515	10	0.512887	10
Et-34	WR	0.703244	30	0.51295	3	03.01.92 (1992)	WR	0.703536	10	0.512880	20
Et-37	WR	0.703332	10			04.1.92 (1992)	WR	0.703547	10	0.512870	10
Et-156	WR	0.703304	10	0.512905	10	16.01.92 (1992)	WR	0.703549	10		
Et-159	WR	0.703075	12	0.512954	14	22.01.92 B (1992)	WR	0.703548	10	0.512877	13
Et-170	WR	0.703164	10	0.512939	10	17.03.92 (1992)	WR	0.703548	10	0.512873	10
Et-173	WR	0.703153	10	0.512955	15	19.04.92 (1992)	WR	0.703551	10		
						19.05.92 (1992)	WR	0.703518	10		
Valle del Bove Volcanics						01.06.92 (1992)	WR	0.703489	12		
VBE 001	WR	0.703385	11	0.512902	11	19.06.92 (1992)	WR	0.703504	15	0.512877	10
VBE 004	WR	0.703308	15	0.512889	10	23.07.92 (1992)	WR	0.703532	10		
VBE 007	WR	0.703316	14	0.512893	10	10.09.92 (1992)	WR	0.703520	11	0.512884	10
VBE 009	WR	0.703409	10	0.512887	13	09.10.92 (1992)	WR	0.703531	10		
VBE 028	WR	0.703316	10	0.512875	20	17.11.92 (1992)	WR	0.703548	10		
VBE 029	WR	0.703226	12	0.512931	10	Dec92 (1992)	WR	0.703562	13		
VBE 030	WR	0.703251	14	0.512912	10	23.01.93 (1993)	WR	0.703571	10	0.512867	10
VBE 031	WR	0.703367	13	0.512899	10	CNE03.10.95A (1995)	WR	0.703537	10	0.512882	10
VBE 034	WR	0.703471	20	0.512854	10	CNE03.10.95B (1995)	WR	0.703555	10		
VBE 037	WR	0.703414	12	0.512877	10	CNE09.11.95 (1995)	WR	0.703551	10	0.512879	10
VBE 045	WR	0.703297	12	0.512880	10	CNE20.12.95 (1995)	WR	0.703564	10		
VBE 046	WR	0.703300	15	0.512911	13	CNE23.12.95B (1995)	WR	0.703553	11	0.512871	10
VBE 053	WR	0.703292	10	0.512904	10	CNE23.12.95L (1995)	WR	0.703555	10	0.512874	10
VBE 029	Cpx	0.703208	10	0.512921	10	CNE07.05.96 (1996)	WR	0.703563	11	0.512868	10
VBE 031	Cpx	0.703367	13	0.512901	10	CNE25.07.96 (1996)	WR	0.703515	10	0.512890	10
VBE 037	Cpx	0.703427	10	0.512875	10	CSE12.05.97 (1997)	WR	0.703557	10	0.512879	10
VBN 007	WR	0.703183	10	0.512920	10	BN14.07.97 (1997)	WR	0.703546	11	0.512880	11
VBN 080	WR	0.703270	15	0.512913	10	CSE16.07.97 (1997)	WR	0.703561	10	0.512876	10
VBN 081	WR	0.703251	10	0.512924	10	BN25.11.97 (1997)	WR	0.703559	10	0.512873	10
VBN 088	WR	0.703168	10	0.512925	10	CSE08.01.98 (1998)	WR	0.703554	10	0.512876	11
VBS 010	WR	0.703389	10	0.512889	10	CNE27.03.98 (1998)	WR	0.703564	10	0.512886	10

APPENDIX 1 *Continued*

Sample	Material	$^{87}Sr/^{86}Sr$	± 2 σ_{mean}	$^{143}Nd/^{144}Nd$	± 2 σ_{mean}	Sample	Material	$^{87}Sr/^{86}Sr$	± 2 σ_{mean}	$^{143}Nd/^{144}Nd$	± 2 σ_{mean}
VBS 027	WR	0.703307	10	0.512890	13	VOR 22.07.98 (1998)	WR	0.703563	10	0.512878	11
VBS 069	WR	0.703440	12	0.512895	15	CSE 27.07.98 (1998)	WR	0.703565	11	0.512873	10
VBS 073	WR	0.703437	11	0.512868	10	BN30.07.98 (1998)	WR	0.703557	10	0.512875	10
VBS 098	WR	0.703347	10	0.512900	10	CSE07.02.99 (1999)	WR	0.703547	10	0.512875	10
						CSE09.02.99 (1999)	WR	0.703558	10	0.512874	15
Lavas from parasitic cones						CSE16.03.99 (1999)	WR	0.703552	10	0.512878	14
Et-31	WR	0.70343	4	0.51287	2	BN11.11.99 (1999)	WR	0.703568	10	0.512876	10
Et-42	WR	0.70343	3	0.51289	2	2CSE-26.01.00 (2000)	WR	0.703600	10	0.512870	10
Et-75	WR	0.703695	12	0.512880	10	5CSE-04.03.00 (2000)	WR	0.703593	10	0.512878	10
Et-78	WR	0.703300	10	0.512896	10	23CSE-15.05.00 (2000)	WR	0.703609	11	0.512874	10
Et-87	WR	0.70337	2			40BCSE-24.06.00 (2000)	WR	0.703585	10	0.512877	10
Et-92	WR	0.70341	3			Quota 2300 (2001)	WR	0.703592	10		
Et-94	WR	0.70339	2	0.51290	1	VDL Quota 2100 (2001)	WR	0.703602	11	0.512882	10
1763 W1	WR	0.70335	2			PdL Quota 2700 (2001)	WR	0.703591	12	0.512857	12
1763 M2	WR	0.70335	3	0.51287	3	CSE Scorie (2001)	WR	0.703609	10	0.512887	10
						Quota 1300 (2001)	WR	0.703592	10	0.512868	10
Historic lavas pre-1971						Sapienza D 2150 (2001)	WR	0.703615	10	0.512852	10
e1852	WR	0.703399	11	0.512895	13	et.89.2 (1989)	Cpx	0.703557	12		
e1910	WR	0.703521	10	0.512884	10	et89.5 (1989)	Cpx	0.703540	10		
e1911	WR	0.703461	10	0.512886	14	15.12.91 (1991)	Cpx	0.703456	14		
e1923	WR	0.703406	12	0.512893	10	04.1.92 (1992)	Cpx	0.703547	10		
e1928/2	WR	0.703406	14	0.512907	11	17.03.92 (1992)	Cpx	0.703479	10		
e1928/3	WR	0.703429	10	0.512905	11	19.05.92 (1992)	Cpx	0.703454	10		
e1947	WR	0.703414	11	0.512901	10	19.06.92 (1992)	Cpx	0.703471	10		
e1949	WR	0.703500	12	0.512893	10	23.01.93 (1993)	Cpx	0.703498	10		
e1951	WR	0.703424	11	0.512908	12	CNE23.12.95L (1995)	Cpx	0.703549	12	0.512874	10
e15 (1971)	WR	0.703480	13	0.512880	11	CNE07.05.96 (1996)	Cpx	0.703558	11	0.512876	10
e1852	Cpx	0.703392	10			VOR 22.07.98 (1998)	Cpx	0.703548	12		
e1910	Cpx	0.703454	11			CSE 27.07.98 (1998)	Cpx	0.703552	10		
e1911	Cpx	0.703442	10								
e1923	Cpx	0.703422	14								
e1928/2	Cpx	0.703391	15								
e1928/3	Cpx	0.703449	15								
e1947	Cpx	0.703416	15								
e1949	Cpx	0.703419	10								
e1951	Cpx	0.703439	14								

«Abbreviations: Cpx, clinopyroxene; WR, whole rock. In parentheses is reported the year of eruption. Errors are on the last digits.»

APPENDIX 2

Major- and trace elements data for selected Mt. Etna volcanics

Sample	et 167	et 159	et 037	VBN -081	VBE -007	VBE -006	VBE -034	et 075	et 018	1852 N	e 47	28/07/01 VDL
Rock type	ThB	AB	TB	TB	MU	TR	BE	AB	TB	TB	TB	TB
Major elements (wt.%)												
SiO_2	49.18	48.10	49.39	49.31	52.88	61.02	59.35	47.43	48.54	49.48	47.79	46.84
TiO_2	1.47	1.44	1.36	2.00	1.19	1.29	1.47	1.59	1.60	1.59	1.61	1.78
Al_2O_3	17.20	16.73	18.81	18.50	20.71	16.94	16.93	16.26	19.08	18.52	18.53	16.62
Fe_2O_3	1.15	2.57	0.67	2.54	3.11	2.22	2.58	3.49	3.03	3.62	3.35	3.26
FeO	8.54	6.69	6.92	6.38	3.12	3.32	3.72	7.04	6.34	5.67	6.31	7.19
MnO	0.15	0.15	0.14	0.15	0.13	0.17	0.19	0.20	0.17	0.17	0.17	0.17
MgO	8.73	10.66	7.07	4.20	2.29	1.88	1.79	7.75	4.84	5.35	6.15	5.75
CaO	9.27	8.60	9.52	8.70	7.27	3.43	3.64	11.65	9.58	9.12	10.30	10.53
Na_2O	3.20	3.53	3.68	4.63	5.46	5.95	5.31	2.51	4.16	4.02	3.40	3.63
K_2O	0.35	0.65	1.35	1.82	2.41	2.82	2.85	1.23	1.55	1.58	1.83	2.05
P_2O_5	0.38	0.42	0.58	0.89	0.76	0.45	0.44	0.36	0.45	0.56	0.41	0.51
LOI	0.39	0.45	0.50	0.87	0.68	0.52	1.72	0.50	0.65	0.33	0.15	0.48
Tot.	100.01	99.99	99.99	99.99	100.01	100.01	99.99	100.01	99.99	100.01	100.00	98.81
Trace elements (ppm)												
Sc	25	25	26	17	13	14	12	37	23	23	28	29
V	169	196	235	221	104	88	83	325	180	283	327	302
Cr	363	414	123	9	18	1	1	132	23	27	36	44
Co	45	48	39	32	23	8	7	46	42	37	42	40
Ni	144	245	60	15	11	3	4	54	27	27	34	43
Rb	5.5	13.0	25.0	41	74	66	63	27.0	38	34	46	46
Sr	455	673	1057	1297	1629	896	835	896	1091	1131	1203	1119
Y	21.8	21.6	23.2	27.5	28.7	35	41	25.9	24	29	27.8	28.0
Zr	99	128	161	209	327	196	416	134	205	215	195	194
Nb	17.5	37	50	67	121	104	101	28.1	61	55	43	43
Cs	0.17	0.21	0.44	0.93	1.17	2.56	2.18	0.70	-	0.77	1.00	0.99
Ba	142	294	583	712	1000	1341	1339	468	720	684	640	593
La	19.6	30.6	59	70	102	111	118	39	65	66	56	54
Ce	40	59	111	138	183	210	240	79	126	136	108	105
Pr	4.8	6.8	12.7	15.8	18.7	22.0	24.3	9.5	14.0	14.3	12.6	12.3

APPENDIX 2: *Continued*

Sample	et 167	et 159	et 037	VBN -081	VBE -007	VBE -006	VBE -034	et 075	et 018	1852 N	e 47	28/07/01 VDL
Rock type	ThB	AB	TB	TB	MU	TR	BE	AB	TB	TB	TB	TB
Nd	20.2	26.0	47	61	66	79	84	38	53	51	49	48
Sm	4.7	5.0	8.4	10.2	10.9	12.9	14.1	7.5	8.9	9.5	9.3	9.3
Eu	1.59	1.68	2.41	3.2	2.89	3.6	3.4	2.21	2.73	2.72	2.73	2.77
Gd	4.7	4.9	6.6	8.4	8.1	9.3	9.3	6.1	8.7	7.2	7.4	7.3
Tb	0.74	0.73	0.87	1.08	0.88	1.33	1.43	0.93	1.11	1.09	1.07	1.09
Dy	4.2	4.1	4.8	5.5	5.2	6.8	7.8	4.8	5.9	5.7	5.4	5.6
Ho	0.80	0.78	0.83	0.98	0.88	1.18	1.46	0.92	0.91	1.00	1.01	1.05
Er	2.10	2.01	2.11	2.41	2.58	3.1	3.7	2.32	2.27	2.50	2.58	2.49
Tm	0.31	0.31	0.31	0.35	0.33	0.47	0.49	0.32	0.33	0.36	0.34	0.34
Yb	1.75	1.78	1.71	1.99	2.39	2.51	3.23	1.96	2.03	2.20	2.11	2.14
Lu	0.25	0.24	0.25	0.28	0.34	0.37	0.45	0.29	0.30	0.31	0.32	0.30
Hf	2.48	2.78	3.7	4.7	5.4	5.4	9.1	3.3	4.4	4.9	4.3	4.6
Ta	0.88	1.86	2.42	2.98	5.8	5.2	5.4	1.44	2.57	2.86	2.28	2.26
Pb	1.3	2.7	-	6.8	11.3	13.7	21.3	5.1	6.7	6.3	6.3	6.2
Th	2.22	4.3	-	10.2	17.5	16.3	20.8	5.4	10.0	9.3	7.2	7.0
U	0.49	1.33	-	2.99	5.6	3.5	5.6	1.59	3.0	2.59	2.16	2.06

«Abbreviations: ThB, tholeiitic basalt; AB, alkali basalt; TB, trachybasalt; MU, mugearite; BE, benmoreite; TR, trachyte. - = not determined.» «et167, Biancavilla tholeiite; et159, Paternò neck; et037, Timpa di Acireale; VBN081, Rocca Capra; VBE-007, "Cicirara" lava from the northern wall of Valle del Bove (Ellittico volcano); VBE-006, "foam" lava (Ellittico volcano); VBE-034, pumice fall (Ellittico volcano); Et075, lava flow at the base of Mt. Maletto scoria cone; et018, Mt. Mazzo (front of the 1780 lava flow); 1852N, Zafferana Etnea (1852-53 lava flow); e47, Mt. de Fiore 1 (1974 eruption); 28/07/01 VDL, Valle del Leone (2001 eruption).»

REFERENCES

ALLARD P., CARBONNELLE J., DAJLEVIC D., LE BRONEC J., MOREL P., ROBE M.C., MAURENAS J.M., FAIVRE-PIERRET R., MARTIN D., SABROUX J.C. and ZETTWOOG P. (1991) — *Eruptive and diffuse emissions of CO_2 from Mount Etna.* Nature, **351**, 387-391.

ANDERSON D.L. (2001) — *A statistical test of the two reservoir model for helium isotopes.* Earth Planet. Sci. Lett., **193**, 77-82.

ARMIENTI P., BARBERI F., INNOCENTI F., POMPILIO M., ROMANO R. and VILLARI L. (1984) — *Compositional variation in the 1983 and other recent Etnean lavas: insights on the shallow feeding system.* Bull. Volcanol., **47**, 995-1007.

ARMIENTI P., INNOCENTI F., PETRINI R., POMPILIO M. and VILLARI L. (1988) — *Sub-aphyric alkali basalt from Etna: inferences on depth and composition of the source magma.* Rend. Soc. It. Mineral. Petrol., **43**, 877-891.

ARMIENTI P., CLOCCHIATTI R., D'ORAZIO M., INNOCENTI F., PETRINI R., POMPILIO M. TONARINI S. and VILLARI L. (1994) — *The long-standing 1991-1993 Mount Etna eruption: petrography and geochemistry of lavas*: Acta Vulcanol., **4**, 15-28.

ARMIENTI P., D'ORAZIO M., INNOCENTI F., TONARINI S. and VILLARI L. (1996) — *October 1995-*

February 1996 Mt. Etna explosive activity: Trace element and isotopic constraints on the feeding system. Acta Vulcanol., **8**, 1-6.

ARMIENTI P., PARESCHI M.T. and POMPILIO M. (1997) — *Lava textures and time scales of magma storage at Mt. Etna (Italy).* Acta Vulcanol., **9**, 1-5.

BEATTIE P.D., FORD C. and RUSSEL. D. (1991) — *Partition coefficients for olivine-melt and orthopyroxene-melt systems.* Contrib. Mineral. Petrol., **109**, 212-224.

CAGGIANELLI A., DEL MORO A., PAGLIONICO G., PINARELLI L. and ROTTURA A. (1991) — *Lower crustal granite genesis connected with chemical fractionation in the continental crust of Calabria (Southern Italy).* Eur. J. Mineral., **3**, 159-180.

CARTER S.R. and CIVETTA L. (1977) — *Genetic implications of the isotope and trace element variations in the eastern sicilian volcanics.* Earth Planet. Sci. Lett., **36**, 168-180.

CHESTER D. (1993) — *Volcanoes and Society.* Edward Arnold, London, 351 pp.

CHESTER D.K., DUNCAN A.N., GUEST J.E. and KILBURN C.R.J. (1985) — *Mount Etna: The anatomy of a volcano.* Cambridge University Press, Cambridge, 404 p.

CHIARABBA C., AMATO A., BOSCHI E. and BARBERI F. (2000) — *Recent seismicity and tomographic modeling of the Mount Etna plumbing system.* J. Geophys. Res., **105**, 10923-10938.

CLOCCHIATTI R., JORON J.L. and TREUIL M. (1988) — *The role of selective alkali contamination in the evolution of recent historic lavas of Mt. Etna.* J. Volcanol. Geotherm. Res., **34**, 241-249.

CLOCCHIATTI R., WEISZ J., MOSBAH M. and TANGUY J.C. (1992) — *Coexistence de «verres» alkalins et tholéiitiques saturés en CO_2 dans les olivines des hyaloclastites d'Aci Castello (Etna, Sicile, Italie). Arguments en faveur d'un manteau anormal et d'un réservoir profond.* Acta Vulcanol., Marinelli Volume, **2**, 161-173.

COLTELLI M., CORSARO R., DEL CARLO P., DEL NEGRO C., GABBIANELLI G., GAMBERINI F., LANZAFAME G., NEGRI A., POMPILIO M., SANGIORGI F., TABACCO S. and VEZZOLI L. (1997) — *Crociera ET97: primi contributi per la realizzazione di una carta batimorfologica e geologica della base sottomarina dell'Etna (Mar Ionio occidentale).* Forum Italiano di Scienze della Terra, Volume 2: Bellaria, Federazione Italiana di Scienze della Terra, 232-234.

CONDOMINES M., TANGUY J.C., KIEFFER G. and ALLEGRE C.J. (1992) — *Magmatic evolution of a volcano studied by ^{230}Th-^{238}U disequilibrium and trace elements systematics: the Etna case.* Geochim. Cosmochim. Acta, **46**, 1397-1416.

CONDOMINES M., TANGUY J.C. and MICHAUD V. (1995) — *Magma dynamics at Mt Etna: Constraints from U-Th-Ra-Pb radioactive disequilibria and Sr isotopes in historical lavas.* Earth Planet. Sci. Lett., **132**, 25-41.

D'ORAZIO M. (1993) — *Natura ed evoluzione delle vulcaniti dell'Etna e loro relazioni con il magmatismo ibleo.* PhD Thesis, Università di Pisa.

D'ORAZIO M. (1995) — *Trace element determination in igneous rocks by ICP-MS: results on ten international reference samples.* Per. Mineral., **64**, 315-328.

D'ORAZIO M., TONARINI S., INNOCENTI F. and POMPILIO M. (1997) — *Northern Valle del Bove volcanic succession (Mt. Etna, Sicily): petrography, geochemistry and Sr-Nd isotope data.* Acta Vulcanol., **9**, 73-86.

DOGLIONI C., INNOCENTI F. and MARIOTTI G. (2001) — *Why Mt. Etna?.* Terra Nova, **13**, 25-31.

FARNETANI C.G., RICHARDS M.A. and GHIORSO M.S. (1996) — *Petrological models of magma evolution and deep crustal structure beneath hotspot and flood basalt province.* Earth Planet. Sci. Lett., **143**, 81-94.

GHIORSO M.S. and CARMICHAEL I.S.E. (1987) — *Modeling magmatic systems: petrologic applications.* - In: Thermodynamic modeling of geological materials: minerals, fluids and melts, Carmichael, I.S.E. and Eugster, H.P. (Eds.), Reviews in Mineralogy, Miner. Soc. Am., **17**, 467-499.

GHIORSO M.S., CARMICHAEL I.S.E. RIVERS M.L. and SACK R.O. (1983) — *The Gibbs free energy of mixing of natural silicate liquids; an expanded regular solution approximation for the calculation of magmatic intensive variables.* Contrib. Mineral. Petrol., **84**, 107-145.

GHIORSO M.S., HIRSCHMANN M.M., REINERS P.W. and KRESS III V.C. (2002) — *The pMELTS: A revision of MELTS for improved calculation of phase relations and major element partitioning related to partial melting of the mantle to 3 GPa.* Geochem. Geophys. Geosyst., **3**, 10.1029/2001GC000217.

GILLOT P.Y., KIEFFER G. and ROMANO R. (1994) — *The evolution of Mount Etna in the light of potassium-argon dating.* Acta Vulcanol., **5**, 81-87.

GRAHAM D., GIACOBBE A., SPERA F. and TILTON G. (1992) — *Chemical and Isotopic Variations in Historical Lavas from Mount Etna.* EOS, AGU Fall Meeting Abs. Suppl., 611.

GVIRTZMAN Z. and NUR A. (1999) — *The formation of Mount Etna as the consequence of slab rollback.* Nature, **401**, 782-785.

HIRN A., NICOLICH R., GALLART J., LAIGLE M., CERNOBORI L. and GROUP E.S. (1997) — *Roots of*

Etna volcano in faults of great earthquakes. Earth Planet. Sci. Lett., **148**, 171-191.

HOFMANN A.W. (1988) — *Chemical differentiation of the Earth: the relationship between mantle, continental crust, and oceanic crust*. Earth Planet. Sci. Lett., 90, 297-314.

HUGHES J.W., GUEST J.E. and DUNCAN A.M. (1990) — *Changing styles of effusive eruption on Mount Etna since AD 1600*. - In: Magma Transport and Storage, Ryan, M.P. (Ed.), John Wiley & Sons Ltd, 385-406.

ISHIKAWA T. and TERA F. (1999) — *Two isotopically distinct fluid components involved in the Mariana arc: Evidence from Nb/B ratios B, Sr, Nd and Pb isotope systematics*. Geology, **27**, 83-86.

JORON J.L. and TREUIL M. (1984) — *Etude géochimique et pétrogènese des laves de l'Etna, Sicile (Italie)*. Bull. Volcanol., **47**, 1125-1144.

KAMENETSKY V. and CLOCCHIATTI R. (1996) — *Primitive magmatism of Mt. Etna: insights from mineralogy and melt inclusions*. Earth Planet. Sci. Lett., **142**, 553-572.

LAIGLE M. and HIRN A. (1999) — *Explosion-seismic tomography of a magmatic body beneath Etna: volatile discharge and tectonic control of volcanism*. Geophys. Res. Lett., **26**, 2665-2668.

LE MAITRE R.W. (2002) — *Igneous rocks - A classification and glossary of terms*. Cambridge University Press, Cambridge, 236 pp.

LONGARETTI G. and ROCCHI S. (1992) — *Il magmatismo dell'avanpaese ibleo (Sicilia orientale tra il Trias e il Quaternario: dati stratigrafici e petrologici del sottosuolo*. Mem. Soc. Geol. It., **45**, 1-17.

MARTY B., TRULL T., LUSSIEZ P., BASILE I. and TANGUY J.C. (1994) — *He, Ar, O, Sr and Nd isotope constraints on the origin and evolution of Mount Etna magmatism*. Earth Planet. Sci. Lett., **126**, 23-39.

MAZZARINI F. and ARMIENTI P. (2001) — *Flank cones at Mount Etna Volcano; do they have a power-law distribution?* Bull. Volcanol., **62**, 420-430.

MCDONOUGH W.F. and SUN S.S. (1995) — *The composition of the Earth*. Chem. Geol., **120**, 223-253.

MÉTRICH,N. and CLOCCHIATTI R. (1989) - *Melt inclusions investigations on the volatile behavior in historic alkali basaltic magmas of Etna*. Bull. Volcanol., **51**, 185-198.

MÉTRICH N. and RUTHERFORD M.J. (1998) — *Low pressure crystallization paths of H_2O-saturated basaltic-hawaiitic melts from Mt. Etna: Implications for open-system degassing of basaltic volcanoes*. Geochim. Cosmochim. Acta, **62**, 1195-1205.

MURRU M., MONTUORI C., WYSS M. and PRIVITERA E. (1999) — *The locations of magma chambers at Mt. Etna, Italy, mapped by b-values*. Geophys. Res. Lett, **26**, 2553-2556.

PATANÈ D., DE GORI P., CHIARABBA C. and BONACCORSO A. (2003) — *Magma ascent and the pressurization of Mount Etna's volcanic system*. Science, **299**, 2061-2063.

PEARCE T.H. (1978) — *Olivine fractionation equation for basaltic and ultrabasic liquids*. Nature, **276**, 771-774.

SCHIANO P., CLOCCHIATTI R., OTTOLINI L. and BUSÁ T. (2001) — *Transition of mount Etna lavas from mantle-plume to an island-arc magmatic source*, Nature, **412**, 900-904.

TANGUY J.C. (1978) — *Tholeiitic Basalt Magmatism of Mount Etna and Its Relations With the Alkaline Series*. Contrib. Mineral. Petrol., **66**, 51-67.

TANGUY J.C. and CLOCCHIATTI R. (1984) — *The Etnean lavas, 1977-1983: petrology and mineralogy*. Bull. Volcanol., **47**, 879-894.

TANGUY J.C., CONDOMINES M. and KIEFFER G. (1997) — *Evolution of Mount Etna magma: Constraints on the present feeding system and eruptive mechanism*. J. Volcanol. Geotherm. Res., **75**, 221-250.

TATSUMI Y. and KOGISO T. (1997) — *Trace element transport during dehydration processes in the subducted oceanic crust: 2. Origin of chemical and physical characteristics in arc magmatism*. Earth Planet. Sci. Lett., **148**, 207-221.

TONARINI S., ARMIENTI P., D'ORAZIO M. and INNOCENTI F. (2001) — *Subduction-like fluids in the genesis of Mt. Etna magmas: evidences from boron isotopes and fluid mobile elements*. Earth Planet. Sci. Lett., **192**, 471-483.

TONARINI S., ARMIENTI P., D'ORAZIO M., INNOCENTI F., POMPILIO M. and PETRINI R. (1995) — *Geochemical and isotopic monitoring of Mt Etna 1989-93 eruptive activity: bearing on the shallow feeding system*. J. Volcanol. Geotherm. Res., **64**, 95-115.

TRIGILA R., SPERA F.J. and AURISICCHIO C. (1990) — *The 1983 Mount Etna eruption: thermochemical and dynamical inferences*. Contrib. Mineral. Petrol., **104**, 594-608.

TRUA T., ESPERANÇA S. and MAZZUOLI R. (1998) — *The evolution of the lithospheric mantle along the N. African Plate: geochemical and isotopic evidence from the tholeiitic and alkaline volcanic rocks of the Hyblean Plateau, Italy*. Contrib. Mineral. Petrol., **131**, 307-322.